Proceedings of the 9ICEG
9th International Congress on Environmental Geotechnics
25-28 June, 2023 | Chania, Greece
© Authors: All rights reserved, 2023
https://doi.org/10.53243/ICEG2023-15

Elasto-viscoplastic constitutive model for time-dependent consolidation characteristics of methane hydrate-bearing sands

K. Nakashima[1], and Y. Nakata[2]

[1]*Assistant professor, Kindai University, Higashiosaka, Japan, email: knakashima@civileng.kindai.ac.jp*

[2]*Professor, Yamaguchi University, Ube, Japan, email: nakata@yamaguchi-u.ac.jp*

ABSTRACT

Methane gas production from methane hydrate reservoirs is expected to become a new technology for natural energy supplies. As an effective technology associated with the methane gas production, the "depressurization method" has been proposed, and several production tests employing depressurization have been achieved in recent years. Due to the accompanying changes in complex stress state during gas production, understanding and evaluating mechanical properties, assuming time-dependency of methane hydrate bearing sediments, is essential. In this study, an elasto-viscoplastic constitutive model that can simulate time-dependent behavior of methane hydrate bearing-sands was proposed based on the experimental results obtained by consolidation tests. Proposed constitutive model introduced the concept that irrecoverable strain was represented as the total of plastic strain and creep strain. The creep strain was described by introducing the logarithmic creep law. Creep parameters need to input depending on the magnitude of confining stress and stress rate. The proposed constitutive model can comprehensively predict time-dependent characteristics, such as stress rate dependent behavior and creep behavior, during consolidation.

Keywords: Methane hydrate, consolidation, creep, elasto-viscoplastic constitutive model

1 INTRODUCTION

Securing fuel resources is issue that needs to be urgently addressed. Methane hydrate (MH) is widely distributed in marine and permafrost regions and is expected to become a future alternative energy resource (Waite et al., 2009). In Japan, MH distribution in the eastern Nankai Trough is confirmed, and offshore production tests were carried out in 2013 and 2017 (Yamamoto et al., 2019).

Depressurization is an efficient technology for producing methane gas from the MH reservoir (Yoneda et al, 2019). During the process of drilling boreholes and the methane gas production, prediction of the complex geotechnical phenomena, such as consolidation and shear deformation of the sediments, is needed. Therefore, it is essential to reveal the mechanical properties of MH-bearing sand (MHBS) for safe gas production. Over the decades, several laboratory studies using gas hydrate-bearing sand (GHBS) have been performed. Gas hydrates exhibit viscous properties, whereby GHBS exhibits time-dependent behavior during shearing, such as strain rate dependency (Miyazaki et al., 2011) and creep deformation (Yoshimoto et al., 2022). The consolidation characteristics of GHBS have recently been investigated. It has been confirmed that the existence of hydrates inhibits the compressibility of the soil (Nakashima et al., 2021). Additionally, MHBS exhibits larger creep deformation during consolidation compared to the hydrate free sands. For safe and economical gas production, development of analysis model that can simulate the geotechnical behavior of GHBS is necessary, and hence, a constitutive model is essential to accurately predict their mechanical properties. Along with the experimental studies, some constitutive models have been proposed in the last decade. However, very few constitutive models have the ability to predict the creep behavior during consolidation.

In this study, an elasto-viscoplastic constitutive model, considering the time-dependent characteristics, was proposed based on the results of consolidation tests on artificial MHBS specimens under various loading conditions.

2 OVERVIEW OF ISOTROPIC CONSOLIDATION TESTS

2.1 Temperature-controlled high-pressure triaxial compression testing apparatus

In this experimental study, a temperature-controlled, high-pressure triaxial compression testing apparatus was employed. This testing apparatus can simulate the in-situ environment of the deep seabed by controlling pore pressure and temperature. Figure 1 shows a schematic diagram of the testing apparatus. The description of its components was comprehensibly outlined in previous reports (Hyodo et al., 2013).

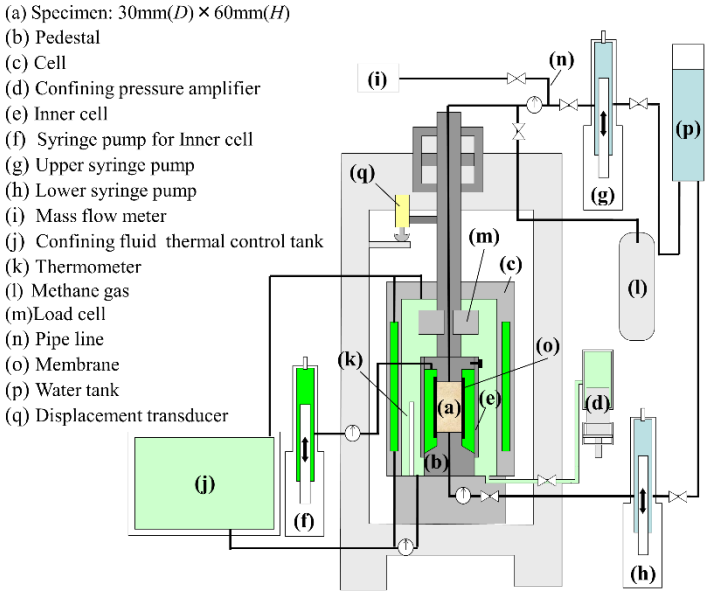


Figure 1. *Schematic diagram of testing apparatus*

2.2 Test material and specimen preparation

Test material that simulated the marine sediments in the eastern Nankai Trough was artificially prepared based on previous investigation results of the natural core materials (Suzuki et al., 2009). Silica sand, silica fines, kaolin and mica were mixed to replicate the minerals and grain size distribution of the MH concentrated sediment layers in the eastern Nankai Trough. Figure 2 shows the particle size distribution curve of the test material.

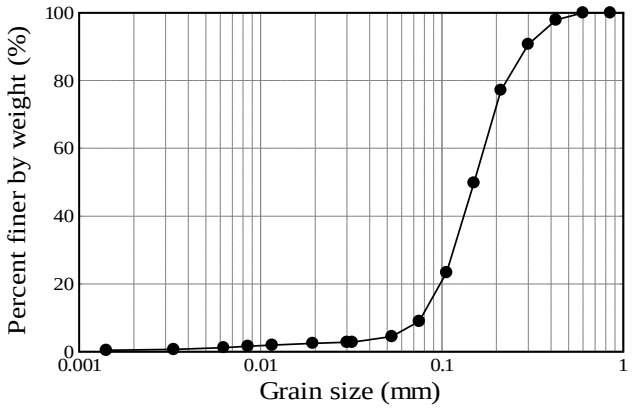


Figure 2. *Particle size distribution curve of artificial sample*

An artificial MHBS specimen was prepared according to the following procedure. Precalculated water and the test material were homogeneously mixed and were tamped in 15 layers by tamping in a mold measuring 30mm in diameter by 60mm in height. Previous study confirmed that the porosity of natural core samples retrieved from the eastern Nankai Trough is between 40~50% (Yoneda et al., 2015). Therefore, the initial target porosity of all specimens was set at 45%. The specimen was installed on a

pedestal in the triaxial cell. Pore pressure and confining pressure were then increased while methane gas was injected into the specimen. The rate of gas injection was not constant, was carefully injected so that the effective stress was not negative. Because the pressure-temperature condition in the cell simulated an environment where MH could be stable, MHs were generated within the soil. After MH generation, the specimen was saturated with water. After the prescribed back pressure was applied, the isotropic consolidation test was conducted. For comparison, the consolidation tests were conducted on the specimen with or without MH.

2.3 Test conditions for isotropic consolidation test

Test conditions for isotropic consolidation tests are summarized in Table 1. In the case of incremental loading consolidation tests, confining pressures was applied to the specimen in steps from 0.2 to 20MPa, and then unloaded in steps from 20 to 0.1MPa. In each step, the confining pressure was held for 1 hour. For monotonic loading consolidation tests, confining pressures from 0.2MPa to 7MPa were simultaneously applied, and the test was conducted with a different stress rate of 0.2, or 2.0MPa/min.

Table 1. *Test conditions*

Case ID	Loading method	Back pressure (MPa)	Temperature T (℃)	Porosity n (%)	Degree of MH saturation S_{MH} (%)	Remarks
IC-1	Incremental loading	5	20	45.9	0.0	
IC-2		5	1	45.3	38.5	
IC-3		5	1	45.6	43.5	
MC-1	Monotonic loading	5	20	45.0	0.0	Stress rate 0.2MPa/min
MC-2		5	1	45.0	47.6	
MC-3		5	20	44.8	0.0	Stress rate 2.0MPa/min
MC-4		5	1	44.8	63.3	

3 ELASTO-VISCOPLASTIC CONSTITUTIVE MODEL FOR METHANE HYDRATE-BEARING SEDIMENTS

The proposed constitutive model is described based on the modified Cam-clay model, and was developed considering the experimental results of the consolidation test (Nakashima et al., 2021).

3.1 Basic relation

The strain rate tensor (stretching), D_{ij}, is assumed to be decomposed into elastic stretching, D^e_{ij}, plastic stretching, D^p_{ij}, and creep stretching, D^c_{ij}, by introducing the theory of the elasto-viscoplastic constitutive model proposed by Hashiguchi and Okayasu (2000).

$$D_{ij} = D^e_{ij} + D^p_{ij} + D^c_{ij} \tag{1}$$

Elastic stretching is expressed using Yang's modulus, E, and Poisson's ratio, ν, as follows.

$$D^e_{ij} = \frac{1+\nu}{E} d\sigma'_{ij} - \frac{\nu}{E} d\sigma'_{kk} \delta_{ij} \tag{2}$$

Where, δ_{ij} indicates Kronecker's delta. Plastic stretching is assumed by the following equation in an accordance with the non-associate flow rule.

$$D^p_{ij} = \Lambda \frac{\partial g}{\partial \sigma'_{ij}} \tag{3}$$

Where, g is the plastic potential, and Λ is the proportionality factor that determines the magnitude of plastic stretching. Creep stretching, expressing time-dependency behavior, is assumed as follows:

$$D_{ij}^{c} = \Lambda^{c} \frac{\partial g^{c}}{\partial \sigma'_{ij}} \tag{4}$$

Where, g^c is the creep potential, and Λ^c is the proportionality factor that determines the magnitude of creep stretching. A mean effective principal stress, p', and a deviator stress, q, are generally described as,

$$p' = \frac{1}{3}\sigma'_{ij}\,\delta_{ij} \tag{5}$$

$$q = \left(\frac{2}{3}S_{ij}S_{ij}\right)^{\frac{1}{2}} \tag{6}$$

where, S_{ij} is deviator stress tensor ($S_{ij} = \sigma_{ij} - p'\delta_{ij}$).

3.2 Yield stress of MHBS

Figure 3 represents a diagram of the e-lnp' relationship between host sand (HS) and MHBS. The yield stress of HS, p'_{0HS}, and the void ratio at the yield stress, e_{0HS}, are determined from the isotropic consolidation test with HS.

$$p'_{0HS} = \exp\left(\frac{e_i - e_c + \lambda \ln p'_i - \kappa \ln p_c}{\lambda - \kappa}\right) \tag{7}$$

$$e_{0HS} = e_i - \lambda \ln \frac{p'_{0HS}}{p'_i} \tag{8}$$

Where, λ and κ are compression and swelling index. In this study, the compression index was determined as the inclination of the normal consolidation line (NCL) between 16 MPa and 20 MPa. The swelling index was determined as the inclination of the over consolidation line (OCL) between 10 MPa and 20 MPa. Parameters, e_i and p'_i, are the void ratio and mean principal stress used to determine the NCL for the e-lnp' relationship. Parameters, e_c and p'_c, are the initial void ratio and the initial mean principal stress used in the test. Assuming the compression index can be regarded as a material constant, the normal consolidation line for MHBS is simply represented as parallel to that of HS.

Kasama et al. (2000) proposed internal stress that express the cementation effects as a mean principal stress component. The internal stress is defined as the p' axis intercept of the critical state line. From the results of triaxial shear test, internal stress due to MHs exponentially increases in agreement with the degree of MH saturation;

$$p_{\mathrm{int}} = \xi S_{MH}{}^{\psi} \tag{9}$$

where, ξ and ψ are parameters determined by curve fitting to the test results. From the results of consolidation tests, the relationship between the difference of void ratio on the NCL at a corresponding stress (in this study, p'=20MPa) and the internal stress is expressed as follows;

$$\Delta e = \frac{p_{\mathrm{int}}}{\beta + \gamma\, p_{\mathrm{int}}} \tag{10}$$

where, β and γ are parameters that express the relationship of the yield stress between HS and MHBS. Additionally, Δe is geometrically introduced as;

$$\Delta e = \lambda \ln\left(\frac{p'_{0MHBS}}{p'_{0HS}}\right) - \kappa \ln\left(\frac{p'_{0MHBS}}{p'_{0HS}}\right) \tag{11}$$

From Eq. (10) and Eq. (11), the yield stress of MHBS is expressed as follows:

$$p'_{0MHBS} = \exp\left[\ln p'_{0HS} + \frac{p_{\text{int}}}{(\beta + \gamma p_{\text{int}})(\lambda - \kappa)}\right] \tag{12}$$

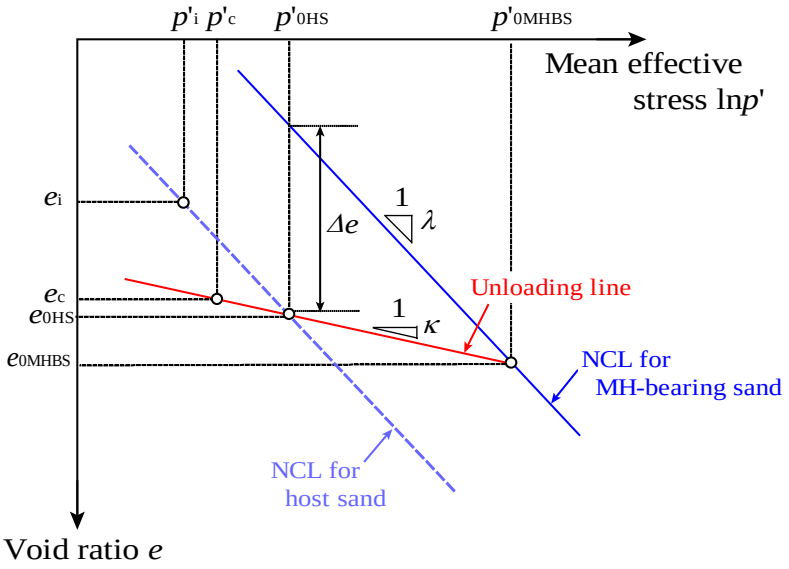


Figure 3. *Diagram of e-lnp' relationship*

3.3 Evaluation of creep stretching

The relationship between creep volumetric strain rate and time during stress holding was plotted on a double-logarithmic scale in Figure 4. As an example, the results of the monotonic loading test are shown. Miyazaki et al. (2011) reported the relationship between creep strain rate and creep time during the shear test is expressed as a straight line, in an accordance with the logarithmic creep law. The results of the stress holding duration of the consolidation test also tend to follow this law. Therefore, the relationship can be given by following formula;

$$\frac{d\varepsilon_v^c}{dt} = D_v^c = D_{v(t0)}^c \cdot \left(\frac{t}{t_0}\right)^{-\alpha} \tag{13}$$

Where, α is a creep coefficient that specifies the gradient of the straight line. $D_{v(t0)}{}^c$ indicates a base creep volumetric strain rate at a specified base time t_0 (in this study, t_0=1sec). Additionally, From Eq.(4), the creep volumetric stretching is expressed as;

$$D_v^c = \Lambda^c tr\frac{\partial g^c}{\partial \sigma'_{ij}} \tag{14}$$

From Eq. (13) and Eq. (14), the creep proportionality factor, Λ_c, can be calculated, and the creep stretching is obtained by its substitution into Eq. (4).

$$D_{ij}^c = D_{v(t0)}^c \left(\frac{t}{t_0}\right)^{-\alpha} \frac{\dfrac{\partial g^c}{\partial \sigma'_{ij}}}{tr\dfrac{\partial g^c}{\partial \sigma'_{ij}}} \tag{15}$$

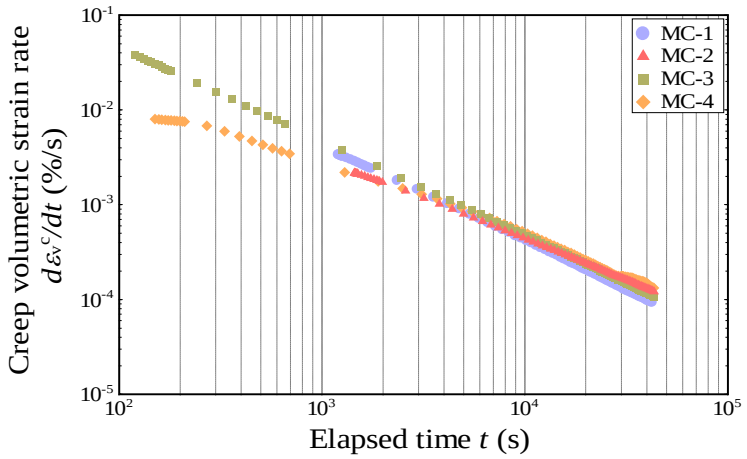


Figure 4. *Creep volumetric strain rate during stress holding*

3.4 Parameter setting

Table 2 shows the parameters input for the analyses. The parameters p_i, e_i, λ, κ. The parameters β, γ, ξ, ψ need to input in the case of MHBS. Creep parameters, α and $D_{v(t0)}{}^c$, need to input depending on the magnitude of confining stress and stress rate.

Table 2. *Parameters for analysis*

Parameters		IC-1	IC-2	IC-3	MC-1	MC-2	MC-3	MC-4
Base mean principle stress (MPa)	p_i			1.00				
Base void ratio	e_i			0.99				
Compression index	λ			0.12				
Swelling index	κ			0.001				
Hardening parameter	β			1.5				
	γ			8.3				
Internal stress parameter	ξ			8.0				
	ψ			3.8				
Time-dependency parameter	α	0.014p'-0.941	0.020p'-0.857		1.00	0.86	1.00	0.72
	$D_v{}^c{}_{(t0)}$	0.015exp(-0.07p')	0.004exp(-0.13p')		0.052	0.014	0.050	0.003

4 SIMULATION OF CONSOLIDATION BEHAVIOR OF METHANE HYDRATE-BEARING SANDS

In this section, the simulation results calculated by the proposed elasto-viscoplastic constitutive model are summarized. The ability of the constitutive model is verified by comparisons with the test results.

Figure 5 shows the relationship between void ratio, e, and mean effective stress, p', during the incremental loading consolidation tests. Comparing HS and MHBS, less fluctuation of void ratio is observed with increasing degree of MH saturation. It can be interpreted that the presence of MHs in pores inhibits soil deformation. During the stress holding, it was also found that the simulation results approximately agreed with the test results.

Subsequently, the results of the monotonic loading consolidation test are presented in Figure 6. An unloading test was not conducted in this consolidation test, and hence, a swelling line was not obtained. As seen by the test results, clear differences in void ratio change emerged depending on the stress rate. For HS, a larger void ratio change emerged in agreement with stress rate. Whereas, for MHBS, less void ratio change can be observed with a higher stress rate. This is because, for HS, the soils were easily compressed corresponding to the stress rate. Whereas, for MHBS, inhibition of compressive deformation is assumed to be due to MHs. The calculated values differ slightly from the experimental

values, yet the constitutive model has the ability to simulate the void ratio change depending on the stress rate. Figure 7 shows the results of the creep volumetric strain that emerged during the stress holding period at each stress rate. A larger creep volumetric strain emerged in MHBS. These results explicitly clarify that MHBS shows remarkable creep behavior. Compared to the simulation results, similar trend to the experimental results was confirmed. However, variation in the volumetric strain prior to the terminate point differ from the experimental results. This is because, in this study, the creep coefficient, α, was specified as the gradient between the initial point and the terminate point during stress holding.

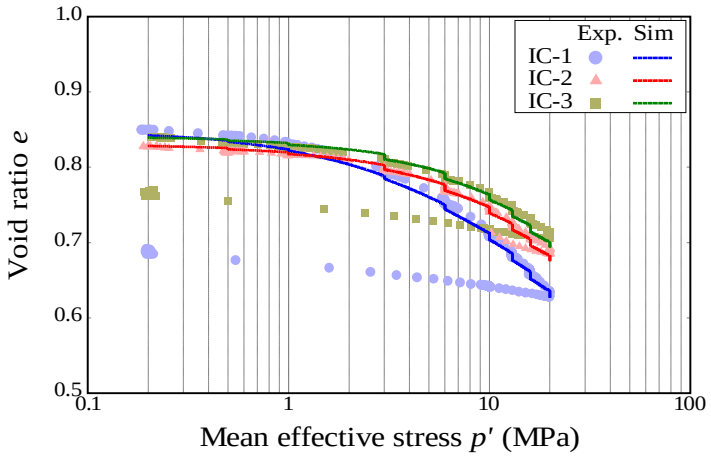
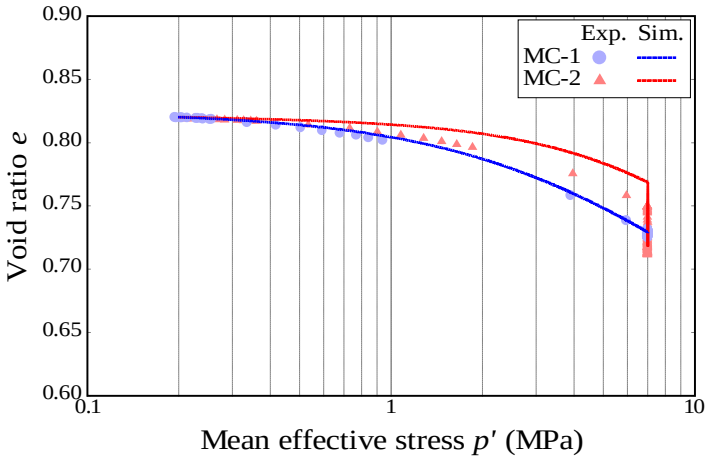
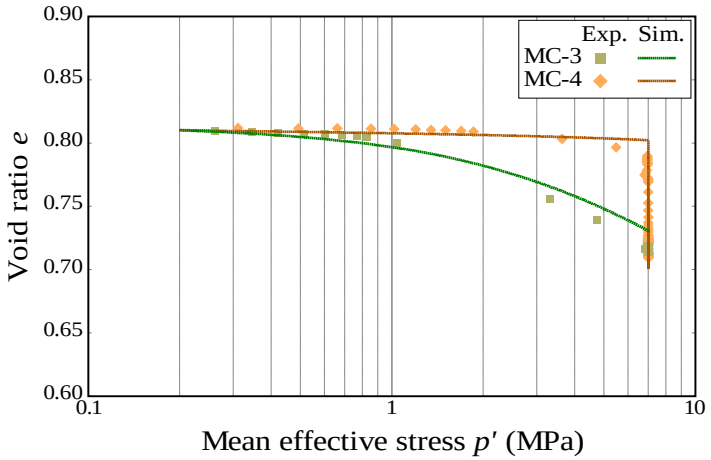


Figure 5. *e-lnp' curve of incremental consolidation test*

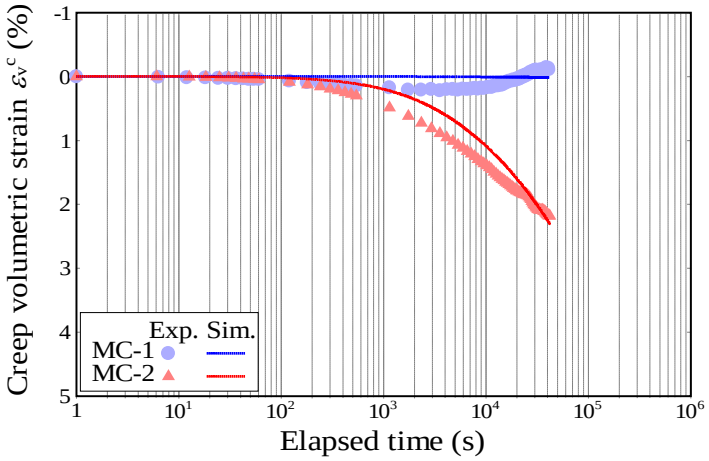


(a) *Stress rate 0.2MPa/min*

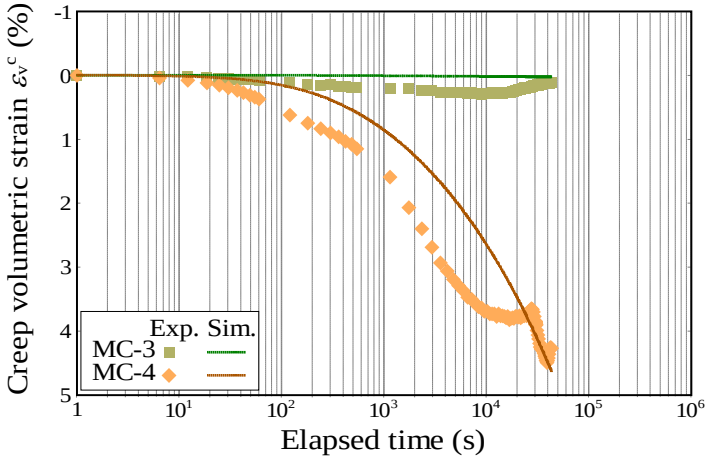


(b) *Stress rate 2.0MPa/min*

Figure 6. *e-lnp' curve of monotonic consolidation test*



***(a)** Stress rate 0.2MPa/min*



***(b)** Stress rate 2.0MPa/min*

***Figure 7.** Creep volumetric strain under monotonic consolidation test*

5 CONCLUSION

In this study, an elasto-viscoplastic constitutive model was proposed based on the results of consolidation tests on artificial MHBS specimens under various loading conditions. Proposed constitutive model introduced the concept that irrecoverable strain was represented as the total of plastic strain and creep strain. Creep volumetric strain rate during stress holding decreased with time, following the logarithmic creep law. The creep stretching was described by introducing this creep law. The proposed constitutive model requires two parameters, α and $D_{v(t0)}{}^c$, to represent time-dependent characteristics of MHBS, such as stress rate dependent and creep behavior, during consolidation. They need to input depending on the magnitude of confining stress and stress rate. The constitutive model showed to comprehensively represent the consolidation behavior under different loading histories.

REFERENCES

Hashiguchi, K., Okayasu, T. (2000). Time-dependent elastoplastic constitutive equation based on the subloading surface model and its application to soils. Soils and Foundations, 40(4), 19-36.

Hyodo, M., Yoneda, J., Yoshimoto, N., Nakata, Y. (2013). Mechanical and dissociation properties of methane hydrate-bearing sand in deep seabed. Soils and Foundations, 53(2), 299-314.

Kasama, K., Ochiai, H., Yasufuku, N. (2000). On the stress-strain behavior of lightly cemented clay based on an extended critical state concept. Soils and Foundations, 40(5), 37-47.

Miyazaki, K., Yamaguchi, T., Sakamoto, Y., Aoki, K. (2011). Time-dependent behaviors of methane-hydrate bearing sediments in triaxial compression test. International Journal of the JCRM, 7(1), 43-48.

Nakashima, K., Nakata, Y., Hyodo, M., Yoshimoto, N., Hiraoka, S., Kajiyama, S. (2021). Compressive characteristics of methane hydrate-bearing sands under isotropic consolidation, Soils and Foundations, 61, 506-519.

Suzuki, K., Ebinuma, T., Narita, H. (2009). Features of Methane Hydrate-bearing Sandy-sediments of the Forearc Basin along the Nankai Trough: Effect on Methane Hydrate-Accumulating Mechanism in Turbidite.

Waite, W. F., Santamarina, J. C., Cortes, D. D., Dugan, B., Espinoza, D. N., Germaine, J., Jang, J., Jung, J. W., Kneafsey, T. J., Shin, H., Soga, K., Winters, W. J., Yun, T. S. (2009). Physical properties of hydrate-bearing sediments. Review of Geophysics, 47, 1-38.

Yamamoto, K., Wang, X.-X., Tamaki, M., Suzuki, K. (2019). The second offshore production of methane hydrate in the Nankai Trough and gas production behavior from a heterogeneous methane hydrate reservoir. RSC Advances, 9, 25987-26013.

Yoneda, J., Masui, A., Konno, Y., Jin, Y., Egawa, K., Kida, M., Ito, T., Nagao, J., Tenma, N. (2015). Mechanical properties of hydrate-bearing turbidite reservoir in the first gas production test site of the Eastern Nankai Trough. Marine and Petroleum Geology, 66, 471-486.

Yoneda, J., Oshima, M., Kida, M., Kato, A., Konno, Y., Jin, Y., Tenma, N. (2019). Consolidation and hardening behavior of hydrate-bearing pressure-core sediments recovered from the Krishna-Godavari Basin, offshore India. Marine and Petroleum Geology, 108, 512-523.

Yoshimoto, M., Kimoto, S. (2022). Undrained creep behavior of CO_2 hydrate-bearing sand and its constitutive modeling considering the cementing effect of hydrates, Soils and Foundations, 62, 101095.